Vortex flow of low concentration NH$_4$Cl–H$_2$O solution during the solidification process

S.Y. Wang, C.X. Lin, M.A. Ebadian*

Florida International University, Hemispheric Center for Environmental Technology, 10555 W. Flager Street, EAS-2100, Miami, FL 33174, USA

Abstract

This paper reports an interesting new phenomenon that occurred during the solidification process of a low-concentration NH$_4$Cl–H$_2$O solution in a rectangular cavity. Vortex flow occurred in the liquid region of the test rectangular cavity during the later stage of the solidification process of the low-concentration NH$_4$Cl–H$_2$O solution. During the solidification process, the vortex flow made the original flow (downward along the vertical frozen surfaces in the liquid region of the test chamber) change and flow upward. The vortex flow was found by using advanced Particle Image Velocimetry (PIV). © 1999 Elsevier Science Ltd. All rights reserved.

1. Introduction

Solid–liquid phase-change (solidification or melting) in multi-component systems occurs in many engineering, environmental, and technology processes, including solidification of castings and ingots, crystal growth, welding, polymer production, freeze-drying of foodstuffs, freezing and melting in oceans, freezing of moist soil, and so on. Phase-change in multi-component systems differs in many respects from solidification or melting of pure substances. Usually, the phase transformation takes place over a temperature range rather than at a discrete temperature. In other words, the solidification phases can coexist at various temperatures, depending on the composition of the mixture. In most multi-component systems, a species also has different solubilities in the liquid and solid phases. Furthermore, during solidification, the solid–liquid interface is not always smooth; a variety of microscopically complicated growth structures can develop (e.g. dendritic or faceted growth). The region characterized by the presence of such an irregular interface is often called a mush zone.

It is now well recognized that natural convection has a considerable influence on the phase-change process in multi-component systems. Both temperature and concentration gradients induce natural convection in the liquid phase. Temperature gradients may be externally imposed (i.e. by heating/cooling of the system) and are generated internally by the release-absorption of the latent heat within the mush zone. Concentration gradients are caused by the preferential incorporation or rejection of a species at the microscopic solid–liquid interface. Because most fluids have vastly different molecular diffusivities for heat and species, a variety of double-diffusive convection patterns can develop in the liquid [1,2]. The present study is concerned with the effects of double-diffusive natural convection on solidification in a binary mixture.

The importance of double-diffusive convection during solidification was first identified in geophysics

---

* Corresponding author. Tel.: +1-305-348-3585; fax: +1-305-348-4176.

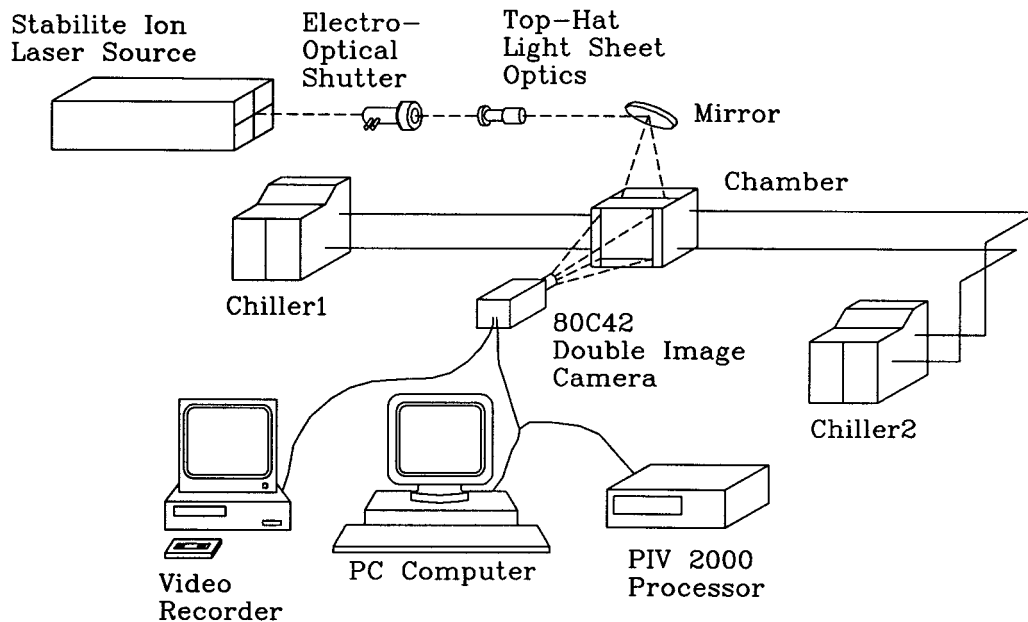*E-mail address:* ebadian@eng.fiu.edu (M.A. Ebadian)

Fig. 1. The PIV velocity measurement system.

and metallurgy, and the experimental studies of Chen and Turner [3] and Szekely and Jassal [4] have provided qualitative features based on flow visualization, such as shadowgraph and dyeing techniques, e.g. salt fingers and sharp diffusive interfaces. Multi-point measurements of temperature and concentration fields during solidification of aqueous solutions have been performed by heat-transfer investigators, such as Beckermann and Viskanta (NH_4Cl–H_2O) [5], Christenson and Incropera (NH_4Cl–H_2O) [6], Okada et al. (NaCl–H_2O) [7], and Nishimura et al. (Na_2CO_3–H_2O) [8,15]. Several years ago, Nishimura and Imoto [9] performed temperature and flow visualization using liquid crystals during solidification of an aqueous solution of NH_4Cl–H_2O in a confined cavity with lateral cooling in order to obtain detailed information on the development of double-diffusive convection through the solidification process. Yet all these results give only some qualitative features of double-diffusive convection during the solidification process. Quantitative features could not be obtained. Because conventional experimental techniques, such as shadowgraph and schlieren, have limits, a detailed picture of double-diffusive convection during the solidification process could not be found. Especially during the later stage of solidification, the flow in the liquid region of the test chamber was very weak; conventional techniques could not measure this extremely slow flow. Recently, the authors studied double-diffusive convection of NH_4Cl–H_2O solution during the solidification process in a rectangular chamber using the Particle Image Velocimetry

(PIV) technique [10,11]; velocity vector plots were obtained from these studies. From these velocity vector plots, more accurate quantitative features have been obtained. Further, an interesting new phenomenon has been found from these tests using PIV. Detailed information on the phenomenon of double-diffusive convection of a NH_4Cl–H_2O solution during the solidification process will be presented below, showing that vortex flow in the liquid region of the test chamber occurred during the solidification process of a low-concentration NH_4Cl–H_2O solution.

2. Experimental system

The schematic of the experimental system is shown in Fig. 1. The test section shown in Fig. 2(a) and (b) is a rectangular enclosure whose inside dimension is 63.5 mm wide, 180 mm high, and 165 mm deep. The 165 mm depth was sufficiently large to render three-dimensional effects negligible. Two vertical cooling walls and the cooling bottom were made of copper plates in which circulating coolant channels were machined. The rest of the walls were made of 12.7-mm-thick plexiglass. Ten type E copper–constantan thermocouples were well distributed on the surface of the copper plates to monitor the surface temperature of the vertical walls of the rectangular enclosure, as shown in Fig. 2(b). To prevent corrosion, the surface of the copper plates was protected with a 25-μm-thick Teflon-based coating. The copper cooling plates were
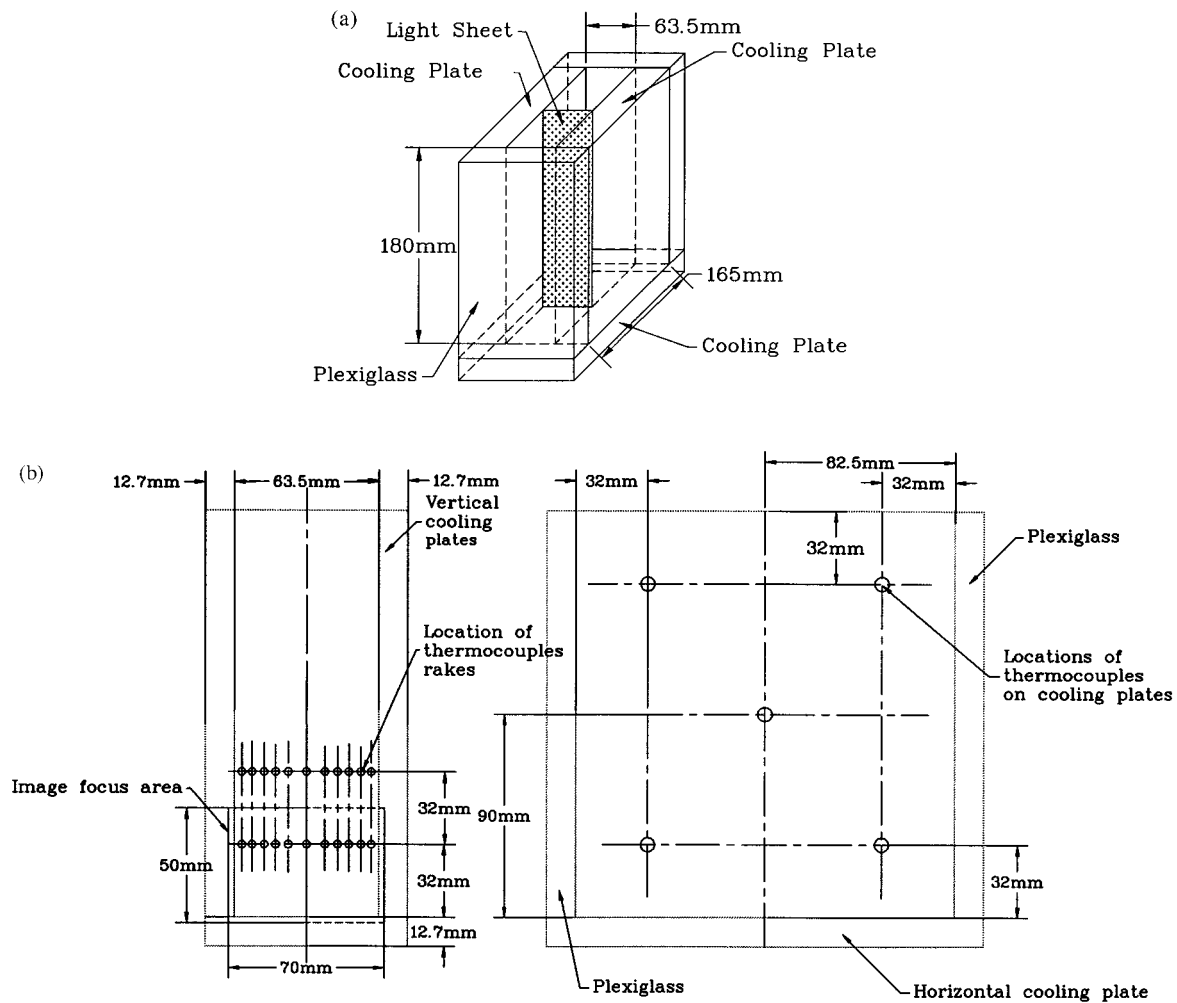
Fig. 2. (a) The test chamber. (b) The locations of thermocouples and image focus areas in test chamber.

chilled with NESLAB HX-540 Recirculating Chiller and NESLAB ULT-90 Recirculating Chiller. One of the chillers initialized the temperature of the solution, and the other one provided the coolant to the test chamber. During the solidification process, a video monitoring system was used to observe the flow phenomena. Temperature distribution in the test solution was obtained by means of the two horizontal rakes, each of which was installed 20 mm away from the rear plate of the test chamber and contained 11 type E copper-constantan thermocouple junctions. The rakes were positioned at two vertical locations within the test chamber, corresponding to elevations of $y = 32$ and 64 mm from the bottom of the chamber as shown in Fig. 2(b). The spacing between thermocouple junctions was staggered, with more junctions installed near the cold walls where large temperature gradients were expected. The output voltages of the thermo-

couples were measured using a LabVIEW data acquisition system, which was controlled by a graphical program written with LabVIEW software and run on a personal computer. The standard limit of uncertainty of type E thermocouples is $\pm 1.7°C$, while the reference junctions in the multiplexes have an uncertainty of $\pm 0.3°C$.

PIV from DANTEC was used to obtain the velocity vector plots containing both velocity amplitude and flow direction for the whole visualized flow field with high accuracy and high resolution. Basically, a PIV system includes four main subsystems: visualization, photographs (cameras), video recordings, and analysis software. A laser is the ideal light source for PIV illumination because of its high intensity, directionality, and easier optical control. For low-speed flows, where only a small area of the flow field is of interest, a shutter-grated, continuous wave laser is used. For this illu-

mination system, the Stabilite® 2017 Ion Laser was used as a continuous wave (CW) laser. The beam from the CW laser was chopped into pulses by DANTEC's 80×41 Electro-Optical Shutter. As with the pulsed laser illumination method, the chopped beam was then expanded by a lens system (e.g. the 80×40 Top-Hat Light-Sheet Optics) to form a pulsing light sheet.

DANTEC's 80C42 DOUBLEImage 700 Camera was used to record images of an illuminated section. The 80C42 DOUBLEImage 700 Camera contains a video format CCD chip and special electronics for fast interframe acquisition of two images. The CCD chip was exposed to scattered light from the first pulse of the light sheet, and the 768×484 pixel image was acquired. The CCD chip was then cleared and exposed to scattered light from the second pulse of the light sheet, and a second full 768×484 pixel image was acquired. Both images were then transferred to DANTEC's PIV 2000 Processor via the digital connector and host computer for data processing and analysis, and the images recorded by the camera were transferred to a video recorder to show flow pattern in the same time.

The 80C42 DOUBLEImage 700 Camera may work in three different modes: (1) double-frame, cross-correlation mode; (2) single-frame, cross-correlation mode; (3) single-frame, auto-correlation mode. By far, it has been claimed, the double-frame cross-correlation mode has the widest application range for flow velocity measurement. In the double-frame mode, one can use cross-correlation to obtain a vector without directional ambiguity with pulse separations anywhere from 66 ms down to 2 μs, allowing measurement of very low up to supersonic speeds. During the solidification of NH_4Cl–H_2O solution in this study, the frozen thickness on the cooling walls of the test chamber continued to increase; the flow of liquid in the test chamber along the frozen surfaces became very weak; and the bulk liquid flow in the middle region of the chamber almost stopped. It was found that the extremely slow flow in the liquid region of the chamber could not be detected by using the double-frame, cross-correlation mode. But for most of the cases examined, the single-frame, cross-correlation mode worked well. This indicated that for the investigation of low-speed flow problems during solidification, vortex flows can be observed when using the single-frame mode and go undetected using double-frame mode. By using the single-frame, cross-correlation mode in this study, some new vortex flow phenomena were identified that were not reported before for the NH_4Cl–H_2O solution. The PIV 2000 Processor is a core part of DANTEC's PIV system and has a modular structure. There are three units that can be inserted into the processor: a correlator unit, input buffers, and a synchronization unit.

In PIV, it is not actually the velocity of the flow that

Table 1
Experimental parameter. D means the double-frame, cross-correlation mode of PIV; S means the single-frame, cross-correlation mode of PIV

Case no.	Initial concentration of solution (wt.%)	Density (kg/m^3) (20°C)	Initial temp. of solution (°C)	Output coolant temp. (°C)[a]	Time between pulses (μs)	Duration of each pulse (μs)	Time between recordings (ms)	Light pulses per recording
1	2	1012.3	23	−22/−26	60,000 (D) 60,000 (S)	3000 (D) 30,000 (S)	20,000 (D) 500 (S)	2 (D) 1 (S)
2	3	1016.3	23	−22/−26	60,000 (D) 60,000 (S)	3000 (D) 30,000 (S)	20,000 (D) 500 (S)	2 (D) 1 (S)
3	3.5	1018.9	23	−22/−26	60,000 (D) 60,000 (S)	3000 (D) 30,000 (S)	20,000 (D) 500 (S)	2 (D) 1 (S)
4	4	1020.8	23	−22/−26	60,000 (D) 60,000 (S)	3000 (D) 30,000 (S)	20,000 (D) 500 (S)	2 (D) 1 (S)
5	5	1024.2	23	−22/−26	60,000 (D) 60,000 (S)	3000 (D) 30,000 (S)	20,000 (D) 500 (S)	2 (D) 1 (S)

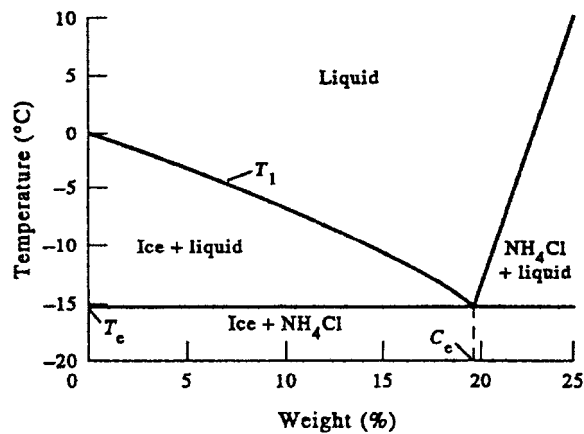[a] −22/−26 means tests were made at two different output coolant temperatures of the chiller.

Fig. 3. Equilibrium phase diagram for NH$_4$Cl–H$_2$O.

is measured, but the velocity of particles suspended in the flow. In this respect, these seeding particles can be considered as probes, and seeding considerations are thus important in PIV. The particles must be small enough to track the flow accurately, yet large enough to scatter sufficient light for the camera to be able to detect them. Ideally, the particles should also be neutrally buoyant in the fluid; that is, they should have approximately the same density as the fluid itself. Strictly speaking, utilizing particles in double-diffusive convection is limited due to the low velocity involved and the density variations present in the fluid. Care should therefore be taken when choosing particles to visualize the convection flow. During the 1970s, to visualize a flow field in double-diffusive convection, Chen et al. [12] reported using aluminum particles in the developed layers formed by heating a stable salinity gradient from a side wall. Huppert and Linden [13] used aluminum particles to observe the structure of flow in a stable solute gradient heated uniformly from below. In this study, the silvered hollow particles made by POTTERS Industries, Inc., which have almost the same density as the solution, were used as the seeding. The density of the solution (or the seeding particle) is provided in Table 1. The diameter of a silvered hollow particle is 10 μm. NH$_4$Cl–H$_2$O solution was used for solidification. The NH$_4$Cl–H$_2$O solution has a eutectic concentration of 19.7%, and the eutectic temperature is −15.4°C. The equilibrium phase diagram for aqueous ammonium chloride is shown in Fig. 3. This solution was selected for several reasons: (1) its semi-transparency, which facilitates flow visualization; (2) its similarity to liquid metal solidification in terms of dendritic growth of the solid phase; (3) the availability of thermophysical property data, which facilitate numerical simulation; and (4) the flexibility that it provides for experimenting magnitude and direction. A major disadvantage of NH$_4$Cl–H$_2$O solution is its

extreme corrosiveness, which significantly reduces the life of test cell components and instrumentation.

As mentioned above, the Stabilite® 2017 Ion Laser was used as a continuous wave (CW) laser; and DANTEC's 80C42 DOUBLEImage 700 Camera was used to record images of an illuminated section, but only a small area of the test chamber can be detected by the camera of the PIV system. The obtained image area or image focus area was 50 × 70 mm, as shown in Fig. 2(b). The detected area, near the bottom of the test chamber, included the two vertical cooling plates and the bottom cooling plate.

3. Results and discussion

To begin the experiment, a solution of desired composition was prepared by mixing the corresponding amount of ammonium chloride and water. After the solution was poured into the chamber, the chiller established the initial temperature of the solution. The depth of the solution in the chamber was 160–170 mm, liquid surface exposed in the atmosphere. After the initial temperature of the solution was established, the coolant with the constant temperature was connected to the test chamber to begin the solidification process.

In previous articles [10,11], the authors reported on the vortex flow of pure water during the solidification process. It is this vortex flow that made the direction of liquid flow along the vertical cooling walls of the test chamber change from flow downward at first to flow upward later. This kind of vortex flow phenomenon occurred during the crystallization of pure water because the density of pure water inverses near 4°C [14], i.e. the density of pure water has its maximum value near 4°C.

The same phenomenon occurred during the solidification process of low-concentration NH$_4$Cl–H$_2$O solution. However, the vortex flow occurred after crystallization, and there was a thicker frozen layer on the cooling walls of the test chamber. The direction of liquid flow along the vertical frozen surfaces of the chamber was also being changed. In the following figures, all flow field results were provided within the bottom area of the rectangular chamber. This was the actual area the PIV system's camera could cover during the experiments. So, the top of each individual drawing in Figs. 4 and 8 was not the top of the actual chamber. Fig. 4 shows a set of velocity vector drawings of 3 wt% NH$_4$Cl–H$_2$O solution during the solidification process. The temperature of output coolant in the chiller was set at −22°C; the other test parameters are shown in Table 1, Case 2. During the first stage of the solidification process, double-frame, cross-correlation mode of the PIV technique was used. The interrogation areas were 32 × 32 pixels. Overlap was

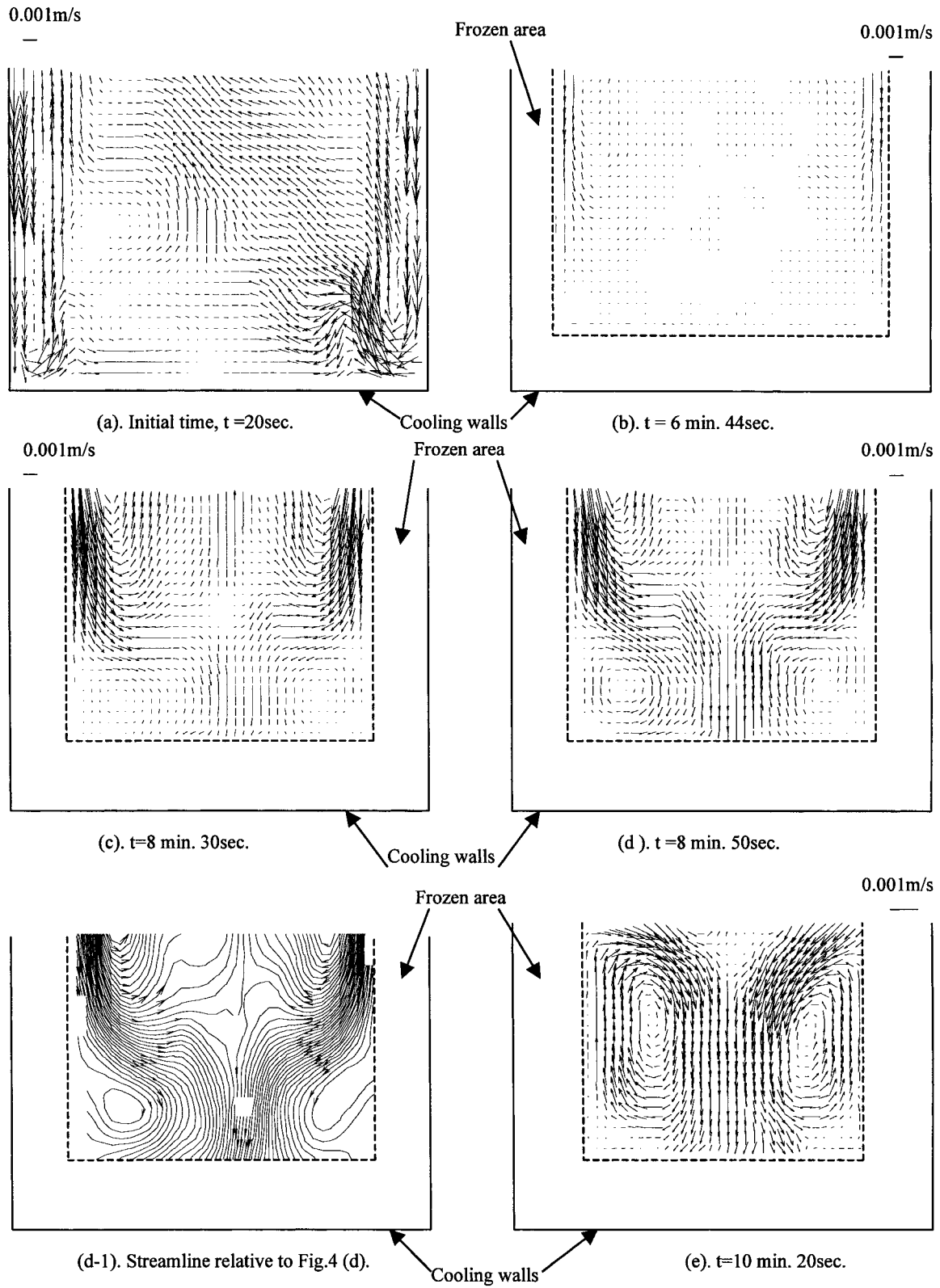Fig. 4. Velocity vector and streamline of 3 wt% NH₄Cl–H₂O solution during solidification process.
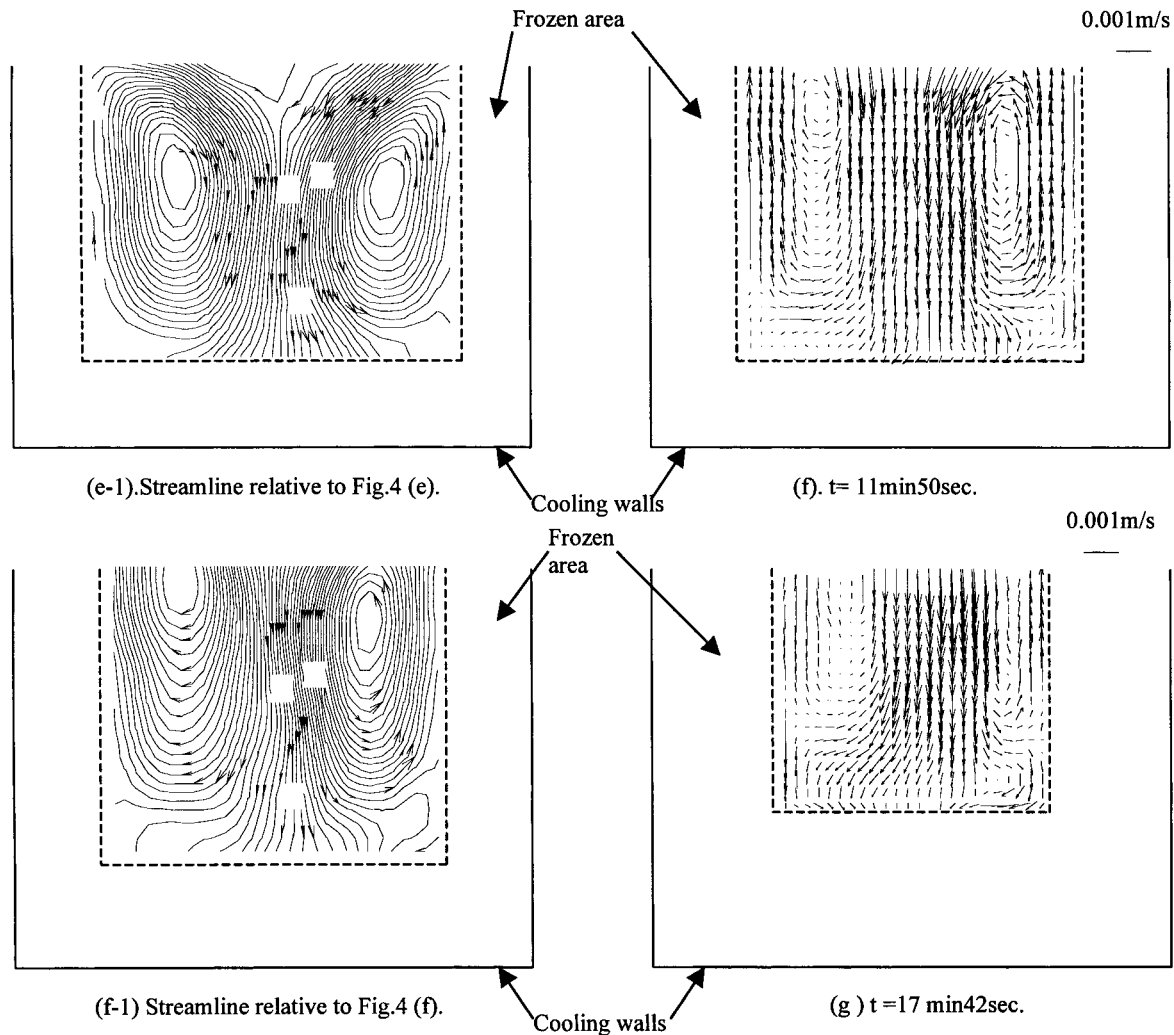
Fig. 4 (*continued*)

Horizontal: 50%, Vertical: 50%. During the later stage of the solidification process, single-frame, cross-correlation mode of PIV was used. The interrogation areas were 32×32 pixels. Overlap was Horizontal: 50%, Vertical: 50%. Fig. 4(a) shows that, at the beginning of the test, the liquid close to the left and right cooling walls flowed downward with a greater velocity because it was directly cooled by the left and right cooling walls. It should be pointed out that the flow in Fig. 4(a) was not asymmetrical. This was because an unstable condition was caused by the two vertical and one horizontal walls that were cooled at the same time. As solidification proceeded, the time-dependent flow between the three walls could not sustain the momentum, which was broken by any small disturbance.

There was a larger temperature gradient in the test solution near the cooling walls. There was also an upward flow at a greater velocity close to the downward flow. The flow in the middle of the chamber was upward. After 6 min 44 s, as shown in Fig. 4(b), the solidification of the NH_4Cl–H_2O solution had proceeded for some time. There was a thicker frozen layer on the cooling walls of the chamber. Because the solidification of the NH_4Cl–H_2O solution with a concentration of 3% by weight is hypoeutectic crystallization, solute-rich liquid was rejected from the interdendritic region. It has a higher density than the bulk liquid, so the solutal buoyancy force enhanced the thermal buoyancy force, and the liquid close to the left and right frozen surfaces flowed downward continuously.

Although the solutal buoyancy force enhanced the thermal buoyancy force, it was greatly reduced for two
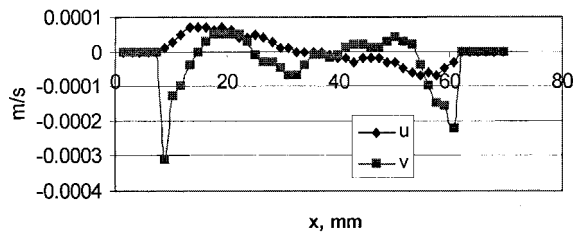
Fig. 5. Velocity plot along the plane of $y = 26$ mm corresponding to the condition of Fig. 4(b).

reasons during the solidification process. First, the convective heat transfer was conducted continuously, and second, the latent heat of crystallization was being released during the solidification of the NH_4Cl–H_2O system. As a result, the flow velocity downward along the vertical frozen surfaces slowed greatly as the solidification proceeded. But it was found that the flow in the chamber middle region was upward during this early period. As shown in Fig. 4(b), the velocity vectors are not clear, especially in the middle of the chamber. This indicates that the double-frame, cross-correlation mode was not able to detect the extremely slow flow in the chamber. Fig. 5 shows the velocity plot, which corresponds to the condition of Fig. 4(b), along a horizontal plane of $y = 26$ mm measured from the bottom of the chamber. From the plot, the maximum velocity is only 0.0003 m/s. The flow in the liquid region of the chamber indeed was extremely slow. The single-frame, cross-correlation mode was used from this time on. As shown in Fig. 4(c), with the solidification of the NH_4Cl–H_2O solution, the frozen thickness on the left and right cooling wall surfaces continued to increase, and the liquid along the frozen surfaces flowed downward continuously, but the flow velocity was slower than that in Fig. 4(a) because the convective heat transfer became conductive gradually. It was interesting to find that vortexes in the opposite direction of early-stage circulating flow zones occurred near the bottom corners of the chamber after Fig. 4(c). These phenomena can be explained by a solute-amassing theory assuming that a maximum condition was reached during the solidification process. With the proceeding of the solidification, a lot of the small dendrites that had formed obstructed liquid flow along the frozen surfaces. The solute-rich liquid was rejected from the interdendritic region during the solidification of 3 wt% NH_4Cl–H_2O solution. The diffusion of the solute NH_4Cl in the solute-rich liquid relied mainly on convection. Because the flow velocity along the vertical frozen surfaces of the chamber was reduced, the solute NH_4Cl that was rejected from the interdendritic region during the solidification process easily amassed in the mush zone and the mush zone–liquid interface. With the solidification process, the amassing of the solute

NH_4Cl became more and more evident, until it reached a maximum. Once that maximum is reached, the amassing of the solute NH_4Cl does not increase again. The solution with a maximum value of solute NH_4Cl flows downward along the vertical frozen surfaces of the chamber and heaps at both corners of the chamber. The solution heaped at the corners has a maximum density; the liquid that flows downward along the frozen surfaces later cannot push the solution because the density of the later liquid is basically the same as or less than that of the solution heaped at the corners. The later liquid not only flowed along the frozen surfaces, but also changed flow direction and flowed to the middle of the chamber, as shown in Fig. 4(c). The solution heaped at the corners was unsteady in movement. The liquid that flowed to the middle of the chamber must drive the seemingly stationary solution heaped at the corners to move. At the same time, the solution heaped at the corners of the chamber was cooled by the vertical and the bottom cooling walls and began crystallization. When the solution layer next to the frozen surfaces crystallized, the latent heat of crystallization was released. The released heat then heats the solution layer next to the just-crystallized layer. The heated solution layer begins to flow upward along the frozen surfaces of the chamber. It also drives the solution heaped at the corners of the chamber to move. The torque produced by the upward force activated on the heaped solution has the same direction as that of the liquid flow to the middle of the chamber. The two driving forces make the solution heaped at the corners of the chamber rotate, that is, form a vortex flow. As Fig. 4(d) shows, with the solidification, the vortex flow becomes stronger and stronger. After 10 min 20 s, as Fig. 4(e) shows, the two vortex flows progress upward close to the vertical frozen surfaces near the corners of the chamber, and the downward solution flow along the left and right frozen surfaces separated from those surfaces. After 11 min 50 s, as Fig. 4(f) shows, the former downward flow along the frozen surfaces has changed direction, but the former vortex flow was retained and extended vertically. After 17 min, 42 s, as Fig. 4(g) shows, the direction of the liquid flowing along the frozen surfaces has basically changed upward as it did in pure water solidification.

Fig. 6 shows the temperature of the cooling walls of the chamber during the 3 wt% NH_4Cl–H_2O solution solidification process. As can be seen from Fig. 6, a rapid drop in wall temperature occurred within the first 5 min. Figs. 7(a) and (b) show the temperature of 3 wt% NH_4Cl–H_2O solution during the solidification process at two chiller output coolant temperature levels. The lower the chiller output temperature, the faster the liquid temperature changes to under 0.0°C.
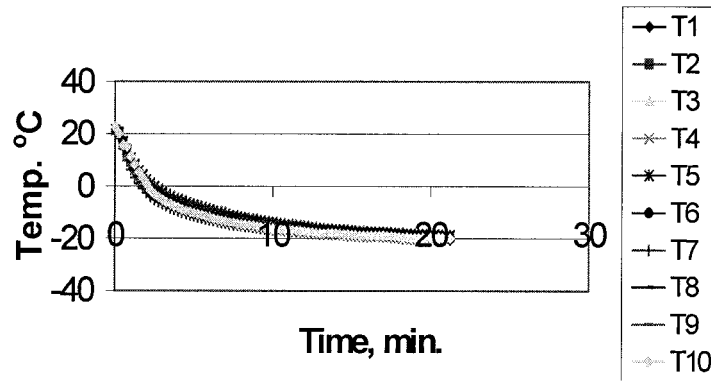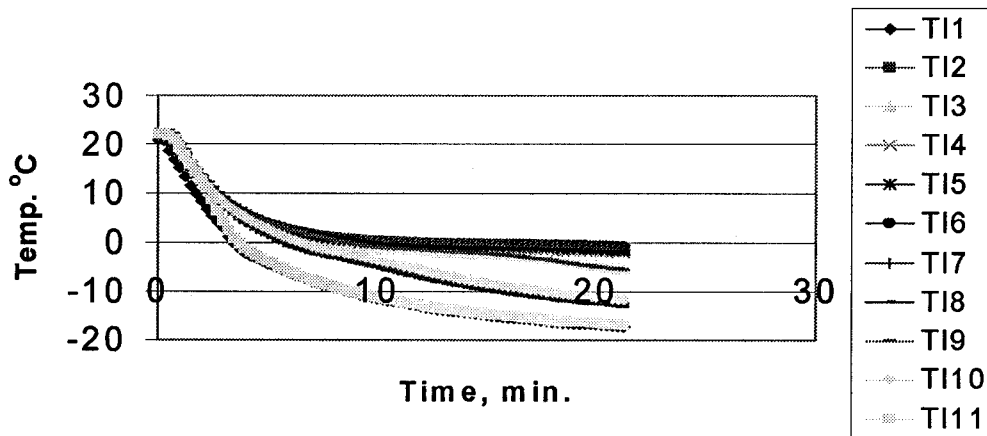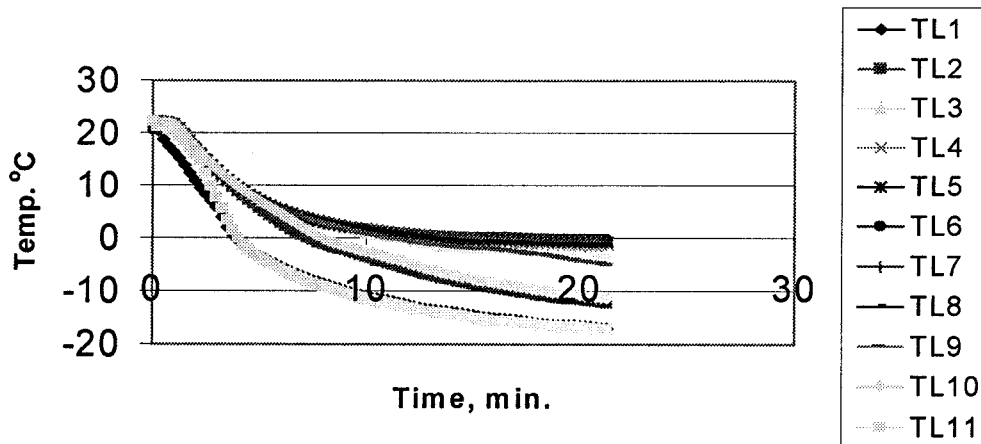
The same vortex flow phenomenon can occur in

Fig. 6. Temperature of cooling walls during 3 wt% NH₄Cl–H₂O solution solidification process.

(a)

(b)

Fig. 7. Temperature of 3 wt% NH₄Cl–H₂O solution during solidification process: (a) output coolant temperature = −26°C; (b) output coolant temperature = −22°C.

other low-concentration NH$_4$Cl–H$_2$O solutions during the solidification process with different concentrations and different temperatures of the output coolant of chiller. The relative test parameters were shown in Table 1. From these tests, it was found that vortex flow could not occur when the concentration of a NH$_4$Cl–H$_2$O solution by weight was greater than 4 wt%.

A set of the flow velocity vector drawings of 5 wt% NH$_4$Cl–H$_2$O solution during solidification process is shown in Fig. 8. The test parameters are shown in Table 1, Case 5. Because the flow patterns of 5 wt% NH$_4$Cl–H$_2$O solution during the earlier stage of solidification were the same as that of 3 wt% NH$_4$Cl–H$_2$O solution, the velocity vectors drawings during the earlier stage of solidification are not shown. Fig. 8(a)

shows that the frozen thickness on the vertical cooling walls of the chamber has evidently increased. The flow in the liquid region of the chamber was extremely slow, and the flow velocity of the liquid region in the chamber almost could not be detected using double-frame, cross-correlation mode of PIV. The velocity vectors drawings shown here were obtained using single-frame, cross-correlation mode of PIV. From Fig. 8(a), the solution along vertical frozen surfaces of the chamber still flowed downward, and there were two almost-steady fluid groups near both corners of the chamber. Fifty-five seconds later, the almost-steady fluid groups still existed, but the vortex flow did not occur, as Fig. 8(b) shows. After 10 min 20 s, as shown in Fig. 8(c), the left almost-steady fluid group does not exist, and the right one has become less clear. The
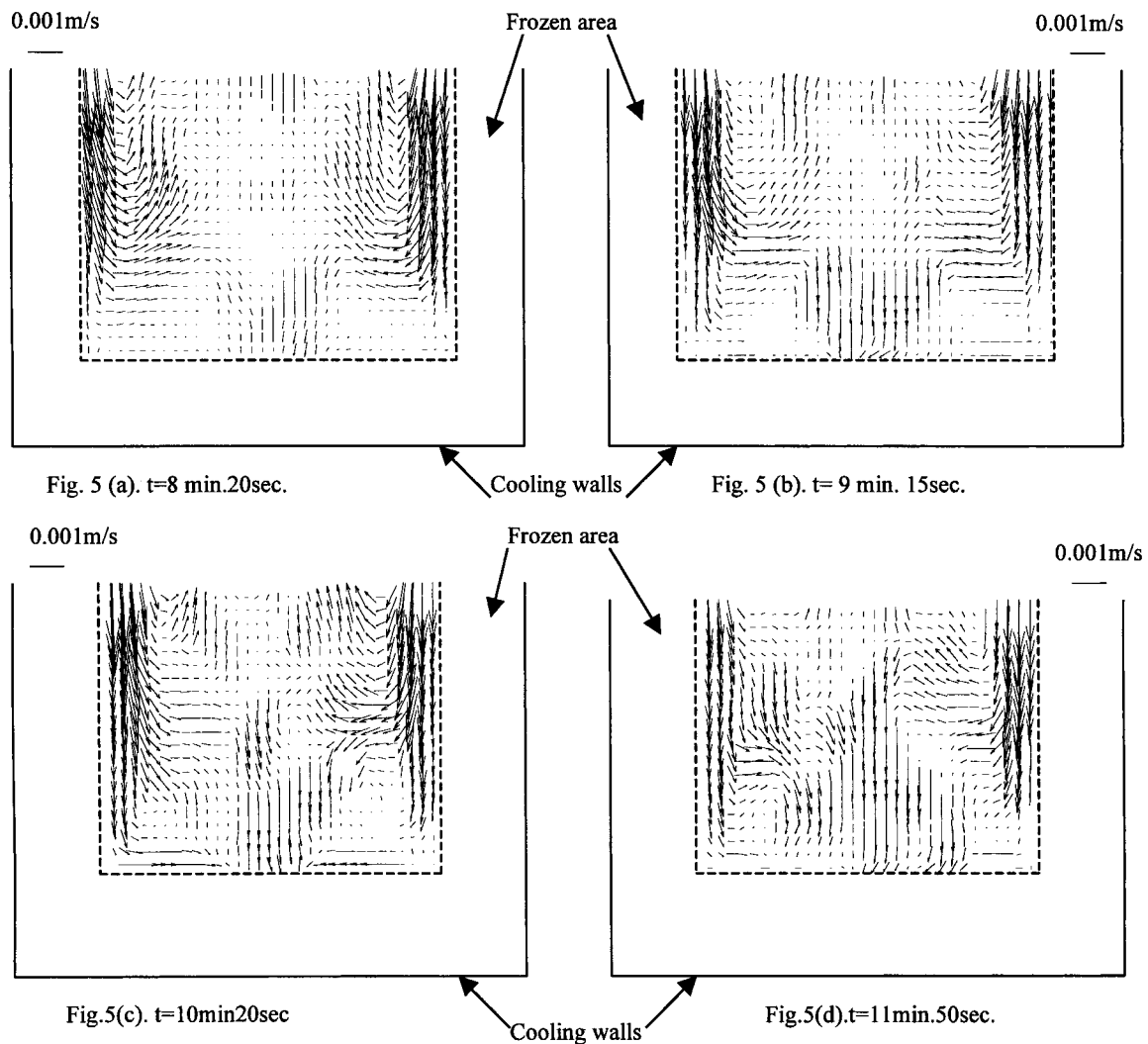

Fig. 8. Velocity vectors of 5 wt% NH$_4$Cl–H$_2$O solution during solidification process.

main flow in the liquid region of the chamber still is the downward flow along the frozen surfaces of the chamber. After 11 min 50 s, as Fig. 8(d) shows, some fluid groups again stayed near the left corner, but vortex flow did not occur, and no fluid groups stayed near the right corner. It is obvious that the vortex flow did not occur during the solidification process of 5 wt% NH_4Cl–H_2O solution. The main reason may be that for the 5 wt% NH_4Cl–H_2O solution, the difference between the initial concentration of NH_4Cl–H_2O solution and that of the solute-rich liquid rejected from the interdendritic region during the solidification process was not big enough to make some solute-rich liquid heap at both corners of the chamber. Therefore, later liquid that flowed downward along the vertical frozen surfaces could not push heaped solute-rich liquid away from the corners and lead to vortex flow.

4. Conclusions

This paper reported an experimental study on the double-diffusive convection of the solidification of a low-concentration NH_4Cl–H_2O solution in a rectangular cavity (chamber). It was found that during the later stage of the solidification of a low-concentration NH_4Cl–H_2O solution, a vortex flow could occur at both corners in the liquid region of the test chamber. With the progress of solidification, the vortex flow also progressed and extended vertically. The vortex flow made the original flow downward along the vertical frozen surfaces of the test chamber in the liquid region change to flow upward. It was also found that when the initial concentration of a low-concentration NH_4Cl–H_2O solution was larger than 4% by weight, the vortex flow did not occur, and if the temperature of the output coolant of the chillers was changed— that is, the strength of cooling was changed—the occurrence of the vortex flow was not influenced.

Through the experimental study, it was found that Particle Image Velocimetry (PIV) is a useful technique. Using PIV, not only was more accurate quantitative information of double-diffusive convection of a binary mixture during solidification process obtained, but detailed information of convection also was obtained that could not be using conventional measurement tools. It is because of the PIV technique that the vortex flow that occurred during the later stage of a low-concentration NH_4Cl–H_2O solution was found.

However, it was also found that the double-frame, cross-correlation mode of PIV was powerless for the extremely slow flow in the liquid region of a low concentration NH_4Cl–H_2O solution during the solidification process in the chamber. The single-frame, cross-correlation mode must be used.

References

[1] H.E. Huppert, J.S. Turner, Double-diffusive convection, J. Fluid Mech. 106 (1981) 229–329.

[2] C.F. Chen, D.H. Johnson, Double-diffusive convection: a report on an Engineering Foundation Conference, J. Fluid Mech. 138 (1984) 405–416.

[3] C.F. Chen, J.S. Turner, Crystallization in a double-diffusive system, J. Geophys. Res. 85 (1980) 2573–2593.

[4] J. Szekely, A.S. Jassal, An experimental and analytical study of the solidification of a binary dendritic system, Metal. Trans. B9 (1978) 389–398.

[5] C. Beckermann, R. Viskanta, Double-diffusive convection during dendritic solidification of a binary mixture, Phys. Chem. Hydrodyn. 10 (1988) 195–213.

[6] M.S. Christenson, F.P. Incropera, Solidification of an aqueous ammonium chloride solution in a rectangular cavity—I. Experimental study, Int. J. Heat Mass Transfer 32 (1989) 47–68.

[7] M. Okada, K. Gotoh, M. Murakami, Solidification of an aqueous solution in a rectangular cell with hot and cold vertical walls, Trans. JSME Ser. B 56 (1990) 1790–1795.

[8] T. Nishimura, M. Fuliwara, H. Miyashita, Double-diffusive convection during solidification of a binary system, Trans. JSME Ser. B 58 (1982) 490–496.

[9] T. Nishimura, T. Imoto, Occurrence and development of double-diffusive convection during solidification of a binary system, Int. J. Heat Mass Transfer 37 (10) (1994) 1455–1464.

[10] S.Y. Wang, Y.Z. Liu, C.X. Lin, M.A. Ebadian, Double-diffusive velocity measurement during the solidification process using particle image velocimetry, in: Proceeding of the ASME Heat Transfer Division, HTD-Vol. 361-4, 1998, pp. 111–118.

[11] S.Y. Wang, C.X. Lin, M.A. Ebadian, Study of double-diffusive velocity during the solidification process using particle image velocimetry. Submitted to Int. J. Heat Mass Transfer, 1998.

[12] C.F. Chen, D.G. Briggs, R.A. Wirtz, Stability of thermal convection in a salinity gradient due to lateral heating, Int. J. Heat Mass Transfer 14 (1971) 57,065.

[13] H.E. Huppert, P.F. Linden, On heating a stable salinity gradient from below, J. Fluid Mech. 95 (3) (1979) 431–464.

[14] T. Nishimura, M. Fuliwara, N. Horie, H. Miyashita, Temperature visualizations by use of liquid crystals of unsteady natural convection during supercooling and freezing of water in an enclosure with lateral cooling, Int. J. Heat Mass Transfer 34 (10) (1991) 2663–2668.

[15] T. Nishimura, M. Fuliwara, H. Miyashita, Double-diffusive convection during solidification of a binary system, Heat Transfer—Jpn. Res. 21 (1992) 586–600.